



Available online at [www.sciencedirect.com](http://www.sciencedirect.com)

SCIENCE @ DIRECT®

International Journal of Solids and Structures 42 (2005) 439–453

INTERNATIONAL JOURNAL OF  
**SOLIDS and**  
**STRUCTURES**

[www.elsevier.com/locate/ijsolstr](http://www.elsevier.com/locate/ijsolstr)

# The effect of the multi-axiality of compressive loading on the accuracy of a continuum model for layered materials

Igor A. Guz \*

*College of Physical Sciences, University of Aberdeen, Fraser Noble Building, King's College, Aberdeen AB24 3UE, Scotland, UK*

Received 19 April 2004

Available online 8 August 2004

---

## Abstract

Two methods of analysis of the internal instability of layered materials are discussed: the continuum approach and the piecewise-homogeneous medium model. Based on the results obtained within the scope of the model of a piecewise-homogeneous medium and the 3-D stability theory, the accuracy of a continuum theory is examined for incompressible non-linear materials undergoing large deformations. Two different loading conditions are compared: biaxial and uniaxial compression. The effect of the multi-axiality of loading on the accuracy of the continuum theory is determined for the particular model of hyperelastic layers described by the Treloar's potential (i.e. by a neo-Hookean type potential), which is a simplified version of the Mooney's elastic potential.

© 2004 Elsevier Ltd. All rights reserved.

**Keywords:** Layered materials; Instability; Compression; Continuum; Non-linear; Large deformation; Homogenisation; Hyperelastic materials; Microstructure

---

## 1. Introduction

Generally speaking, in mechanics of heterogeneous (piecewise-homogeneous) media, there are two major distinctive approaches to describe the behaviour of solids. One of them is based on the model of piecewise-homogeneous medium (Fig. 1a), when the behaviour of each material constituent is described by 3-D equations of solid mechanics provided certain boundary conditions are satisfied at the interfaces. This approach enables to investigate phenomena occurring in the internal microstructure of solids in the most rigorous

---

\* Tel.: +44 122 427 2808; fax: +44 122 427 2519.

E-mail address: [i.guz@abdn.ac.uk](mailto:i.guz@abdn.ac.uk)

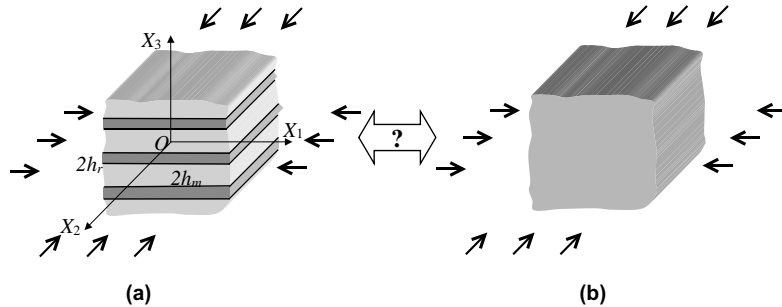


Fig. 1. Model of (a) piecewise-homogeneous medium and (b) continuum theory.

way. However, due to its complexity the method is restricted to a small group of problems. The other approach, or continuum theory (Fig. 1b), involves significant simplifications. Within the continuum theory, the heterogeneous material is simulated by a homogeneous anisotropic material with effective constants, by means of which physical properties of the original material, shape and volume fraction of the constituents are taken into account. The continuum theory may be applied when the scale of the investigated phenomena (for example, the wavelength of the mode of stability loss) is considerably larger than the scale of material internal structure (say, the layer thickness). The approach based on the model of the piecewise homogeneous medium is free from such restrictions and is, therefore, the most accurate one.

The continuum theory, due to its simplicity, is widely used to characterise the mechanical behaviour of composite materials, but questions on its accuracy and domain of applicability always arise. The answer may be given only by comparing the results obtained from the continuum theory to the most accurate approach, i.e. the piecewise-homogeneous medium model. The latter imposes no restrictions on the scale of investigated phenomena and therefore has a much larger domain of applicability. The results obtained within the continuum theory must follow from those derived using the model of a piecewise-homogeneous medium if the ratio between the scale of structure and the scale of phenomenon tends to zero. If this is the case, the continuum theory can be regarded as asymptotically accurate one.

This paper focuses on the behaviour of layered non-linear materials undergoing large deformations compression. The moment of stability loss in the microstructure of the material—internal instability according to Biot (1965)—is treated as the onset of the fracture process. This assumption was suggested for the first time by Dow and Grunfest (1960) and later used in the numerous publications on compressive strength of fibrous or laminated composites; see for example, the reviews by Guz (1990a, 1992), Camponeschi (1991) and Schultheisz and Waas (1996). It is generally recognised that a better understanding of special compression failure mechanisms, specific only to heterogeneous materials, is crucial to the development of improved composite materials. The task of deriving 3-D analytical solutions to describe the compressive response is considered as one of great importance. Such solutions, if obtained, enable us to analyse the behaviour of a structure on the wide range of material properties, and kinematic and loading boundary conditions, without the restrictions imposed by simplified approximate methods.

In this work, two different methods of analysis are compared: the continuum theory and the piecewise-homogeneous medium model. At that, *both* methods employ the rigorously linearised 3-D equations, i.e. the 3-D stability theory (Guz, 1999). The use of 3-D stability theory places the methods into the category of “exact” approaches, as opposed to approximate models based on certain simplifications when describing the stress-strain state.

As applied to the internal instability of fibrous or laminated composites, the exact approach was utilised—probably for the first time—in the late 1960s by A.N. Guz, when the problem for linear-elastic layers

under uniaxial compression was solved within the continuum theory and within the model of a piecewise-homogeneous medium. Later the exact solutions were derived also for more complex problems: for orthotropic, non-linear elastic and elastic-plastic, compressible and incompressible layers including the case of large (finite) deformations—see, for example, Guz (1990a, 1992, 1999), Babich et al. (2001), Tkachenko and Chekhov (2002), Korzh and Chekhov (2002), Guz and Guz (2003) and other publications mentioned there.

Another model of compressive fracture of composites, which is commonly utilised, is based on the investigation of fibre kinking and kink-band formation. It should be briefly mentioned here, although this paper does not analyse the kinking phenomenon. From the literature, it is easy to get the impression that internal instability (microbuckling) and kinking are competing mechanisms. In fact, a kink band is an outcome of the microbuckling failure of actual fibres, as observed experimentally by Guynn et al. (1992). Fibre microbuckling occurs first, followed by propagation of this local damage to form a kink band. Studies of the kinking phenomenon were reviewed, in particular, by Budiansky and Fleck (1994) and Soutis (1996). It was shown by Soutis and Turkmen (1995) that the existing kinking analyses are able to account for some, but not all, of the experimental observations. They correctly predict that shear strength and fibre imperfections are important parameters affecting the compressive strength of the composite. However, within this model it is not possible to say exactly how the strength will vary with fibre content; it requires knowledge of the shear strength properties and the value of misalignment is chosen arbitrarily.

The importance and the complexity of the considered phenomena caused a large number of publications which put forward various approximate methods aimed at tackling the problems with different levels of accuracy—see the reviews by Campaneschi (1991), Budiansky and Fleck (1994), Soutis (1996), Schultheisz and Waas (1996) and Niu and Talreja (2000). It was concluded after the detailed analyses (Guz, 1990a, 1992, 1999; Soutis and Turkmen, 1995; Niu and Talreja, 2000; Soutis and Guz, 2001) that the approximate methods are too simplistic and not very accurate when compared to experimental measurements and observations. For instance, the model proposed by Rosen (1965) involves considerable simplifications, modelling the reinforcement layers by the thin beam theory and the matrix as an elastic material using one-dimensional stress analysis. It makes the results of this method inaccurate even for the simplest case of a composite with linear elastic compressible layers undergoing small pre-critical deformations and considered within the scope of geometrically linear theory. For small fibre volume fractions the approximate approach gives physically unrealistic critical strains. It does not describe the phenomenon under consideration even on the qualitative level, since it predicts a different mode of stability loss from that obtained by the 3-D exact analysis.

For more complex models, which take into account large deformations and geometrical and physical non-linearity (e.g. those considered in this paper), the approximate theories are definitely inapplicable and one can expect even a bigger difference between the exact and approximate approaches. The exact approach, which is used in this paper, is based on the 3-D stability theory and, therefore, allows us to take into account large deformations, geometrical and physical non-linearities and load biaxiality that the simplified methods cannot consider.

The present work examines the continuum theory (Guz, 1990a, 1999) applied to predict the critical instability load in a layered incompressible *non-linear* material undergoing *finite (large) deformations* under *equi-biaxial loading*. The study focuses on how accurate the continuum (homogenised) model describes the internal instability in comparison with the most accurate approach, i.e. the piecewise-homogeneous medium model (Fig. 1a). Special attention is paid to the investigation of the effect of the biaxiality of loading on the continuum theory accuracy.

In the past, investigations of the continuum theory accuracy in relation to the model of piecewise-homogeneous medium were performed only for other physical phenomena, for example, for the problems of wave propagation by Brekhovskikh (1960), or for other models of layers (Guz, 1990b; Guz and

Soutis, 2001a), where the final conclusions were generally limited by the case of small deformations. Besides that, validation of the Cosserat-continuum approach to buckling of linear elastic medium was considered by Papamichos et al. (1990) and Vardoulakis and Sulem (1995), where only numerical solutions by the “transfer matrix technique” for particular layered media were used. The problem for materials under large deformations was studied by Guz and Soutis (2001b) for the case of uniaxial deformation only. However, there are not yet such investigations for the non-axisymmetrical problem of internal instability in non-linear incompressible layered materials under biaxial loading. This paper attempts to fill the gap. Part of the analysis is based on the previous works by the author, so the equations derived earlier are presented only for the clarification purposes without much detail.

## 2. The model of a piecewise-homogeneous medium

### 2.1. General formulation

Let us consider the statement of the static non-axisymmetrical problem of stability for layered materials. At that, a special attention will be paid to accounting for *large* deformations and the *biaxiality* of compressive loads. The material consists of alternating layers with thicknesses  $2h_r$  and  $2h_m$  (Fig. 1a), which are simulated by incompressible non-linear elastic transversally isotropic solids with a general form of the constitutive equations. Henceforth all values referred to these layers will be labelled by indices  $r$  (reinforcement) and  $m$  (matrix). The values of displacement, stress and strain corresponding to the precritical state will be marked by the superscript ‘0’ to distinguish them from perturbations of the same values ( $u_i^0$  and  $u_i$ ,  $\varepsilon_{ij}^0$  and  $\varepsilon_{ij}$ ,  $S_{ij}^0$  and  $S_{ij}$  respectively). Suppose also that the material is undergoing equi-biaxial compression in the plane of the layers by static “dead” loads applied at infinity in such a manner that equal deformations along all layers are provided.

Within the scope of the most accurate approach—i.e. using the piecewise-homogeneous medium model and the equations of the 3-D stability theory (Guz, 1999)—the following eigen-value problem is solved. The axial displacement,  $u_i^0$ , and strain,  $\varepsilon_{ij}^0$  (in terms of the elongation/shortening factor  $\lambda_j$  in the direction of the  $OX_j$  axis) for the considered type of loading can be expressed as

$$u_i^0 = (\lambda_i - 1)x_i, \quad \lambda_i = \text{const}, \quad \varepsilon_{ij}^0 = (\lambda_i - 1)\delta_{ij}. \quad (1)$$

The equations of stability for the individual incompressible layers are (Guz, 1999)

$$\frac{\partial}{\partial x_i} t_{ij}^r = 0, \quad \frac{\partial}{\partial x_i} t_{ij}^m = 0; \quad i, j = 1, 2, 3, \quad (2)$$

The non-symmetrical stress tensor  $t_{ij}$  is referred to the unit area of the relevant surface elements in the undeformed state, which is the reference configuration. This is the non-symmetrical Piola–Kirchhoff stress tensor or nominal stress tensor. Further we shall consider also the symmetrical stress tensor  $S_{ij}$  which reduces to  $\sigma_{ij}$  for the case of small precritical deformations. For incompressible solids, stresses are related to displacements by ( $p$  is hydrostatic pressure)

$$t_{ij} = \kappa_{ij\alpha\beta} \frac{\partial u_\alpha}{\partial x_\beta} + \delta_{ij} \lambda_j^{-1} p. \quad (3)$$

The incompressibility condition has the following form:

$$\lambda_1 \lambda_2 \lambda_3 = 1. \quad (4)$$

The components of the tensor  $\kappa_{ij\alpha\beta}$  depend on the material properties and on the loads (i.e. on the pre-critical state). The quantity characterising the precritical state, i.e. the stress  $S_{ij}^0$ , the strain  $\varepsilon_{ij}^0$  or the elongation/shortening factor  $\lambda_j$ , is the parameter in respect to which the eigen-value problem is solved. In the most general case (Guz, 1999)

$$\kappa_{ij\alpha\beta} = \lambda_j \lambda_\alpha [\delta_{ij} \delta_{\alpha\beta} A_{\beta i} + (1 - \delta_{ij})(\delta_{i\alpha} \delta_{j\beta} \mu_{ij} + \delta_{i\beta} \delta_{j\alpha} \mu_{ji})] + \delta_{i\beta} \delta_{j\alpha} S_{\beta\beta}^0. \quad (5)$$

The particular expressions for  $\kappa_{ij\alpha\beta}$  can be obtained for various kinds of constitutive equations. For example, for hyperelastic solids, if  $\Phi$  is the strain energy density function (elastic potential), then

$$A_{\beta i} = A_{\beta i}(\Phi, \varepsilon_{nl}^0), \quad \mu_{\beta i} = \mu_{\beta i}(\Phi, \varepsilon_{nl}^0). \quad (6)$$

To complete the problem statement, boundary conditions should be written for each interface. For the perfectly bonded layers we have the continuity conditions for the stresses and for the displacements

$$t_{31}^r = t_{31}^m, \quad t_{32}^r = t_{32}^m, \quad t_{33}^r = t_{33}^m, \quad u_3^r = u_3^m, \quad u_2^r = u_2^m, \quad u_1^r = u_1^m. \quad (7)$$

## 2.2. Solutions for two modes of stability loss

The exact solutions of the above-stated 3-D non-axisymmetrical problems of internal instability for incompressible non-linear elastic layers were found by Guz (1989). The characteristic determinants were derived for the case of biaxial compression as applied to four modes of stability loss. Note that the plane problem (uniaxial compression) for such materials was studied in Guz (1992) and Babich et al. (2001).

Solutions of Eq. (2) (i.e. perturbations of stresses and displacements) can be expressed through the functions  $X$  and  $\Psi$  which, in their turn, are the solutions of the following equations (Guz, 1999):

$$\left( \Delta_1 + \xi_1^2 \frac{\partial^2}{\partial x_3^2} \right) \Psi = 0, \quad \left( \Delta_1 + \xi_2^2 \frac{\partial^2}{\partial x_3^2} \right) \left( \Delta_1 + \xi_3^2 \frac{\partial^2}{\partial x_3^2} \right) X = 0, \quad (8)$$

where

$$\xi_1^2 = \frac{\kappa_{3113}}{\kappa_{1221}}, \quad \xi_2^2 = C + \sqrt{C^2 - \lambda_1^6 \frac{\kappa_{3113}}{\kappa_{1331}}}, \quad \xi_3^2 = C - \sqrt{C^2 - \lambda_1^6 \frac{\kappa_{3113}}{\kappa_{1331}}},$$

$$\Delta_1 = \frac{\partial^2}{\partial x_1^2} + \frac{\partial^2}{\partial x_2^2}, \quad C = \frac{\kappa_{3333} + \lambda_1^6 \kappa_{1111} - 2\lambda_1^3 (\kappa_{1133} + \kappa_{1313})}{2\kappa_{1331}}. \quad (9)$$

The parameters  $\xi_j^r$  and  $\xi_j^m$ , which are given by Eq. (9), depend on the components of the tensor  $\kappa_{ij\alpha\beta}$  and, therefore, on the properties of the layers and on the loads. It was proved by Guz (1989) that  $\xi_j^{r^2}$  and  $\xi_j^{m^2}$  are always real and positive. Before proceeding with the construction of solutions for two modes of stability loss (Figs. 2 and 3) we introduce the notations, which will be useful later

$$\alpha_r = \pi h_r l^{-1}, \quad \alpha_m = \pi h_m l^{-1}, \quad l^{-1} = \sqrt{l_1^{-2} + l_2^{-2}}. \quad (10)$$

Here  $l_i$  is the half-wavelength of the modes of stability loss along the  $OX_i$  axis, and  $\alpha$  is the normalised wavelength.

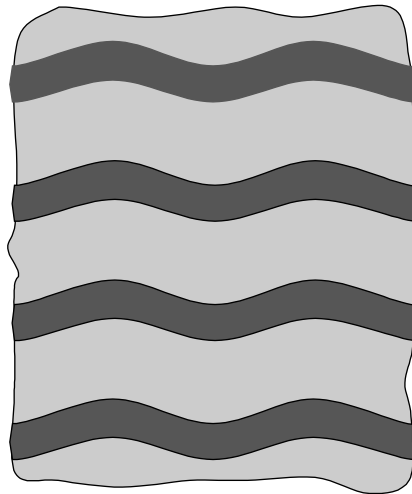


Fig. 2. The first (shear) mode of stability loss.

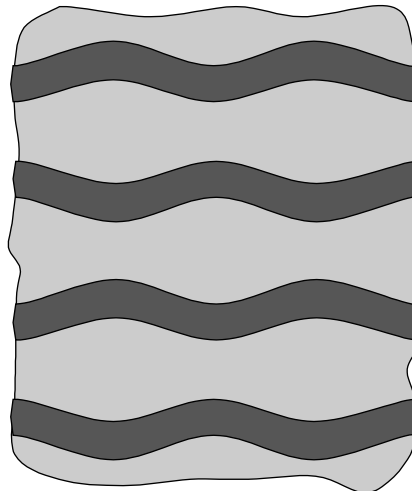


Fig. 3. The second (extensional) mode of stability loss.

For the case of

$$\xi_2^r \neq \xi_3^r, \quad \xi_2^m \neq \xi_3^m \quad (11)$$

the potentials  $X$  and  $\Psi$  can be set up as follows (subscript  $j$  denotes the number of the layer):

- for the first mode (Fig. 2), which is often called anti-symmetrical or shear mode,

$$\begin{aligned}
X_j^r &= \chi^r(\cosh x_3) \equiv \left( A^r \cosh \frac{\pi}{l\xi_2^r} x_3 + B^r \cosh \frac{\pi}{l\xi_3^r} x_3 \right) \sin \frac{\pi}{l_1} x_1 \sin \frac{\pi}{l_2} x_2, \\
\Psi_j^r &= \psi^r(\sinh x_3) \equiv C^r \sinh \frac{\pi}{l\xi_1^r} x_3 \cos \frac{\pi}{l_1} x_1 \cos \frac{\pi}{l_2} x_2, \\
X_j^m &= \chi^m(\cosh x_3) \equiv \left( A^m \cosh \frac{\pi}{l\xi_2^m} x_3 + B^m \cosh \frac{\pi}{l\xi_3^m} x_3 \right) \sin \frac{\pi}{l_1} x_1 \sin \frac{\pi}{l_2} x_2, \\
\Psi_j^m &= \psi^m(\sinh x_3) \equiv C^m \sinh \frac{\pi}{l\xi_1^m} x_3 \cos \frac{\pi}{l_1} x_1 \cos \frac{\pi}{l_2} x_2;
\end{aligned} \tag{12}$$

- for the second mode (Fig. 3), which is often called symmetrical or extensional mode,

$$\begin{aligned}
X_j^r &= \chi^r(\cosh x_3), \quad \Psi_j^r = \psi^r(\sinh x_3), \\
X_j^m &= \chi^m(\sinh x_3), \quad \Psi_j^m = \psi^m(\cosh x_3), \\
X_{j+1}^r &= -\chi^r(\cosh x_3), \quad \Psi_{j+1}^r = -\psi^r(\sinh x_3), \\
X_{j+1}^m &= -\chi^m(\sinh x_3), \quad \Psi_{j+1}^m = -\psi^m(\cosh x_3).
\end{aligned} \tag{13}$$

The components of  $t_{ij}$  and  $u_i$  can be expressed (Guz, 1999) through the potentials  $X$  and  $\Psi$ . Substituting them into the boundary conditions, Eq. (7), which due to the periodicity of both, the material and the solution, are to be satisfied on one interface only, we get the  $(6 \times 6)$  characteristic determinant. This determinant can be analytically reduced to the  $(4 \times 4)$  determinant

$$\det \|\beta_{rs}\| = \begin{vmatrix} \beta_{11} & \beta_{12} & \beta_{13} & \beta_{14} \\ \beta_{21} & \beta_{22} & \beta_{23} & \beta_{24} \\ \beta_{31} & \beta_{32} & \beta_{33} & \beta_{34} \\ \beta_{41} & \beta_{42} & \beta_{43} & \beta_{44} \end{vmatrix} = 0, \quad r, s = 1, 2, 3, 4. \tag{14}$$

The elements of the determinant are given below:

- for the first mode of stability loss (Fig. 2)

$$\begin{aligned}
\beta_{11} &= \left( \lambda_1^{-3} \kappa_{1313}^r + \xi_2^{r-2} \kappa_{3113}^r \right) \cosh \alpha_r \xi_2^{r-1}, \quad \beta_{12} = \left( \lambda_1^{-3} \kappa_{1313}^r + \xi_3^{r-2} \kappa_{3113}^r \right) \cosh \alpha_r \xi_3^{r-1}, \\
\beta_{13} &= \left( \lambda_1^{-3} \kappa_{1313}^m + \xi_2^{m-2} \kappa_{3113}^m \right) \cosh \alpha_m \xi_2^{m-1}, \quad \beta_{14} = \left( \lambda_1^{-3} \kappa_{1313}^m + \xi_3^{m-2} \kappa_{3113}^m \right) \cosh \alpha_m \xi_3^{m-1}, \\
\beta_{21} &= \left( \lambda_1^3 \xi_2^{r-2} \kappa_{2112}^r - \lambda_1^{-3} \kappa_{2222}^r - \lambda_1^3 \kappa_{1111}^r + 2\kappa_{1133}^r + \kappa_{1313}^r \right) \xi_2^{r-1} \sinh \alpha_r \xi_2^{r-1}, \\
\beta_{22} &= \left( \lambda_1^3 \xi_2^{r-2} \kappa_{2112}^r - \lambda_1^{-3} \kappa_{2222}^r - \lambda_1^3 \kappa_{1111}^r + 2\kappa_{1133}^r + \kappa_{1313}^r \right) \xi_3^{r-1} \sinh \alpha_r \xi_3^{r-1}, \\
\beta_{23} &= \left( \lambda_1^3 \xi_2^{m-2} \kappa_{2112}^m - \lambda_1^{-3} \kappa_{2222}^m - \lambda_1^3 \kappa_{1111}^m + 2\kappa_{1133}^m + \kappa_{1313}^m \right) \xi_2^{m-1} \sinh \alpha_m \xi_2^{m-1}, \\
\beta_{24} &= \left( \lambda_1^3 \xi_3^{m-2} \kappa_{2112}^m - \lambda_1^{-3} \kappa_{2222}^m - \lambda_1^3 \kappa_{1111}^m + 2\kappa_{1133}^m + \kappa_{1313}^m \right) \xi_3^{m-1} \sinh \alpha_m \xi_3^{m-1}, \\
\beta_{31} &= \xi_2^{r-1} \sinh \alpha_r \xi_2^{r-1}, \quad \beta_{32} = \xi_3^{r-1} \sinh \alpha_r \xi_3^{r-1}, \quad \beta_{33} = \xi_2^{m-1} \sinh \alpha_m \xi_2^{m-1}, \\
\beta_{34} &= \xi_3^{m-1} \sinh \alpha_m \xi_3^{m-1}, \quad \beta_{41} = \cosh \alpha_r \xi_2^{r-1}, \quad \beta_{42} = \cosh \alpha_r \xi_3^{r-1}, \\
\beta_{43} &= \cosh \alpha_m \xi_2^{m-1}, \quad \beta_{44} = \cosh \alpha_m \xi_3^{m-1};
\end{aligned} \tag{15}$$

- for the 2nd mode of stability loss (Fig. 3)

$$\begin{aligned}
\beta_{11} &= \left( \lambda_1^{-3} \kappa_{1313}^r + \xi_2^{r-2} \kappa_{3113}^r \right) \cosh \alpha_r \xi_2^{r-1}, \quad \beta_{12} = \left( \lambda_1^{-3} \kappa_{1313}^r + \xi_3^{r-2} \kappa_{3113}^r \right) \cosh \alpha_r \xi_3^{r-1}, \\
\beta_{13} &= \left( \lambda_1^{-3} \kappa_{1313}^m + \xi_2^{m-2} \kappa_{3113}^m \right) \sinh \alpha_m \xi_2^{m-1}, \quad \beta_{14} = \left( \lambda_1^{-3} \kappa_{1313}^m + \xi_3^{m-2} \kappa_{3113}^m \right) \sinh \alpha_m \xi_3^{m-1}, \\
\beta_{21} &= \left( \lambda_1^3 \xi_2^{r-2} \kappa_{2112}^r - \lambda_1^{-3} \kappa_{2222}^r - \lambda_1^3 \kappa_{1111}^r + 2\kappa_{1133}^r + \kappa_{1313}^r \right) \xi_2^{r-1} \sinh \alpha_r \xi_2^{r-1}, \\
\beta_{22} &= \left( \lambda_1^3 \xi_3^{r-2} \kappa_{2112}^r - \lambda_1^{-3} \kappa_{2222}^r - \lambda_1^3 \kappa_{1111}^r + 2\kappa_{1133}^r + \kappa_{1313}^r \right) \xi_3^{r-1} \sinh \alpha_r \xi_3^{r-1}, \\
\beta_{23} &= \left( \lambda_1^3 \xi_2^{m-2} \kappa_{2112}^m - \lambda_1^{-3} \kappa_{2222}^m - \lambda_1^3 \kappa_{1111}^m + 2\kappa_{1133}^m + \kappa_{1313}^m \right) \xi_2^{m-1} \cosh \alpha_m \xi_2^{m-1}, \\
\beta_{24} &= \left( \lambda_1^3 \xi_3^{m-2} \kappa_{2112}^m - \lambda_1^{-3} \kappa_{2222}^m - \lambda_1^3 \kappa_{1111}^m + 2\kappa_{1133}^m + \kappa_{1313}^m \right) \xi_3^{m-1} \cosh \alpha_m \xi_3^{m-1}, \\
\beta_{31} &= \xi_2^{r-1} \sinh \alpha_r \xi_2^{r-1}, \quad \beta_{32} = \xi_3^{r-1} \sinh \alpha_r \xi_3^{r-1}, \quad \beta_{33} = \xi_2^{m-1} \cosh \alpha_m \xi_2^{m-1}, \\
\beta_{34} &= \xi_3^{m-1} \cosh \alpha_m \xi_3^{m-1}, \quad \beta_{41} = \cosh \alpha_r \xi_2^{r-1}, \quad \beta_{42} = \cosh \alpha_r \xi_3^{r-1}, \\
\beta_{43} &= \sinh \alpha_m \xi_2^{m-1}, \quad \beta_{44} = \sinh \alpha_m \xi_3^{m-1}.
\end{aligned} \tag{16}$$

Similarly, the characteristic equations can be derived for other modes of stability loss. The proposed method can also give the solutions for other modes. However, based on the experience of solving similar problems for other properties of layers for the case of small deformations (Guz, 1990a,b, 1992; Babich et al., 2001; Guz and Soutis, 2001a; Soutis and Guz, 2001) and the plane problems (Guz and Soutis, 2001b), the modes with the larger periods are not of practical interest.

### 3. Asymptotic analysis

The continuum theory may be applied when the scale of the investigated phenomena (i.e. the wavelength of the mode of stability loss  $2l$ ) is considerably larger than the scale of material internal structure (i.e. the layer thickness  $2h$ ). If the results obtained within the continuum theory follow from those derived using the model of a piecewise-homogeneous medium when the ratio between the scale of structure and the scale of phenomenon tends to zero, i.e. when

$$hl^{-1} \rightarrow 0, \tag{17}$$

the continuum theory can be regarded as asymptotically accurate one.

In this section the asymptotic analysis of the solutions obtained in the previous section within the piecewise-homogeneous medium model will be performed. For this purpose, the limits are calculated analytically under the condition given by Eq. (17). Under this condition, Eq. (10) yield

$$\alpha_r \rightarrow 0, \quad \alpha_m \rightarrow 0, \tag{18}$$

and, therefore,

$$\begin{aligned}
\cosh \frac{\alpha_r}{\xi_2^r} &\rightarrow 1, \quad \cosh \frac{\alpha_m}{\xi_2^m} \rightarrow 1, \quad \sinh \frac{\alpha_r}{\xi_2^r} \rightarrow \frac{\alpha_r}{\xi_2^r}, \quad \sinh \frac{\alpha_m}{\xi_2^m} \rightarrow \frac{\alpha_m}{\xi_2^m}, \\
\cosh \frac{\alpha_r}{\xi_3^r} &\rightarrow 1, \quad \cosh \frac{\alpha_m}{\xi_3^m} \rightarrow 1, \quad \sinh \frac{\alpha_r}{\xi_3^r} \rightarrow \frac{\alpha_r}{\xi_3^r}, \quad \sinh \frac{\alpha_m}{\xi_3^m} \rightarrow \frac{\alpha_m}{\xi_3^m}.
\end{aligned} \tag{19}$$

After substitution of Eq. (19) into Eq. (14) and a number of rearrangements, the characteristic equations are reduced to the following form:

- for the first mode (Fig. 2), from Eqs. (14), (15) and (19),

$$\frac{(\xi_2^{r-2} - \xi_3^{r-2})(\xi_2^{m-2} - \xi_3^{m-2})\pi^2}{l^2 \lambda_1^3} \times \left[ \frac{h_m}{h_r} (\kappa_{1313}^m - \kappa_{1313}^r)^2 - \left( \frac{h_m}{h_r} \kappa_{1331}^m + \kappa_{1331}^r \right) \left( \kappa_{3113}^m + \frac{h_m}{h_r} \kappa_{3113}^r \right) \right] = 0; \quad (20)$$

- for the second mode (Fig. 3), from Eqs. (14), (16) and (19),

$$(\xi_2^{r-2} - \xi_3^{r-2})(\xi_2^{m-2} - \xi_3^{m-2})(\xi_2^m \xi_3^m)^{-1} \lambda_1^3 \kappa_{3113}^m \kappa_{3113}^r = 0. \quad (21)$$

It was shown [36] the inequalities

$$\kappa_{3113}^r > 0, \quad \kappa_{3113}^m > 0 \quad (22)$$

always hold for any material. Also, as was mentioned before, for the considered models of layers the parameters  $(\xi_j^r)^2$  and  $(\xi_j^m)^2$  are always real and positive. Therefore, taking into account Eqs. (11) and (22), the characteristic equation, which corresponds to the second (extensional) mode, i.e. Eq. (21), does not have non-trivial solutions. Of course, the characteristic equation for this mode might have roots within the most accurate approach, i.e. within the model of piecewise-homogeneous medium, Eq. (14). The example of the second mode having roots will be given later in Fig. 4.

On the contrary, Eq. (20), which corresponds to the first mode of stability loss, can have roots within the continuum approximation. For the further analysis, the components of tensor  $\kappa_{ij\alpha\beta}$  can be expressed (Guz, 1999) as

$$\begin{aligned} \kappa_{3113}^r &= \lambda_1^2 \mu_{13}^r, & \kappa_{131}^r &= \lambda_1^{-4} \mu_{13}^r + (S_{11}^0)^r, & \kappa_{1313}^r &= \lambda_1^{-1} \mu_{13}^r, \\ \kappa_{3113}^m &= \lambda_1^2 \mu_{13}^m, & \kappa_{131}^m &= \lambda_1^{-4} \mu_{13}^m + (S_{11}^0)^m, & \kappa_{1313}^m &= \lambda_1^{-1} \mu_{13}^m. \end{aligned} \quad (23)$$

Substitution of Eqs. (23) into the characteristic equation for the first mode, Eq. (20), gives

$$\lambda_1^{-2} \frac{h_m}{h_r} (\mu_{13}^m - \mu_{13}^r)^2 - \left[ \lambda_1^{-2} \mu_{13}^r + \lambda_1^{-2} \frac{h_m}{h_r} \mu_{13}^m + \lambda_1^2 \left( (S_{11}^0)^r + \frac{h_m}{h_r} (S_{11}^0)^m \right) \right] \left( \mu_{13}^m + \frac{h_m}{h_r} \mu_{13}^r \right) = 0. \quad (24)$$

In order to analyse Eq. (24), the effective values of stresses and of quantity  $\mu_{13}$ , denoted respectively as  $\langle S_{11}^0 \rangle$  and  $\langle \mu_{13} \rangle$ , will be utilised. At the moment of material stability loss, they can be calculated by well-known formulae as

$$\langle S_{11}^0 \rangle = (S_{11}^0)^r V_r^* + (S_{11}^0)^m V_m^*, \quad \langle \mu_{13} \rangle = \mu_{13}^r \mu_{13}^m (\mu_{13}^r V_m^* + \mu_{13}^m V_r^*)^{-1}, \quad (25)$$

where  $V_r^*$  and  $V_m^*$  are the volume fractions of the components in the deformed state. Due to the kind of applied loads, Eq. (1), the volume fractions of the components in the non-deformed ( $V_r, V_m$ ) and the deformed states ( $V_r^*, V_m^*$ ) are equal for the same components:

$$V_r^* = \frac{\lambda_2^r h_r}{\lambda_3^r h_r + \lambda_3^m h_m} = \frac{h_r}{h_r + h_m} = V_r, \quad V_m^* = \frac{\lambda_2^m h_m}{\lambda_3^r h_r + \lambda_3^m h_m} = \frac{h_m}{h_r + h_m} = V_m. \quad (26)$$

Let us denote the theoretical strength limit as  $(\Pi_1^-)_T$ . Substitution of Eqs. (25) and (26) into Eq. (24), after some rearrangement, yields

$$(\Pi_1^-)_T \equiv -\langle S_{11}^0 \rangle = \lambda_1^{-4} \langle \mu_{13} \rangle. \quad (27)$$

This coincides with the results derived within the scope of the continuum theory (Guz, 1990a, 1999) as applied to non-linear incompressible layered materials undergoing large deformations.

Thus, it is rigorously proved for layered non-linear elastic materials undergoing large deformations in equi-biaxial compression that the results of the continuum theory follow as a long-wave approximation from those for the first mode of stability loss obtained using the model of piecewise-homogeneous medium. Therefore, the asymptotic accuracy of the continuum theory for such materials is established.

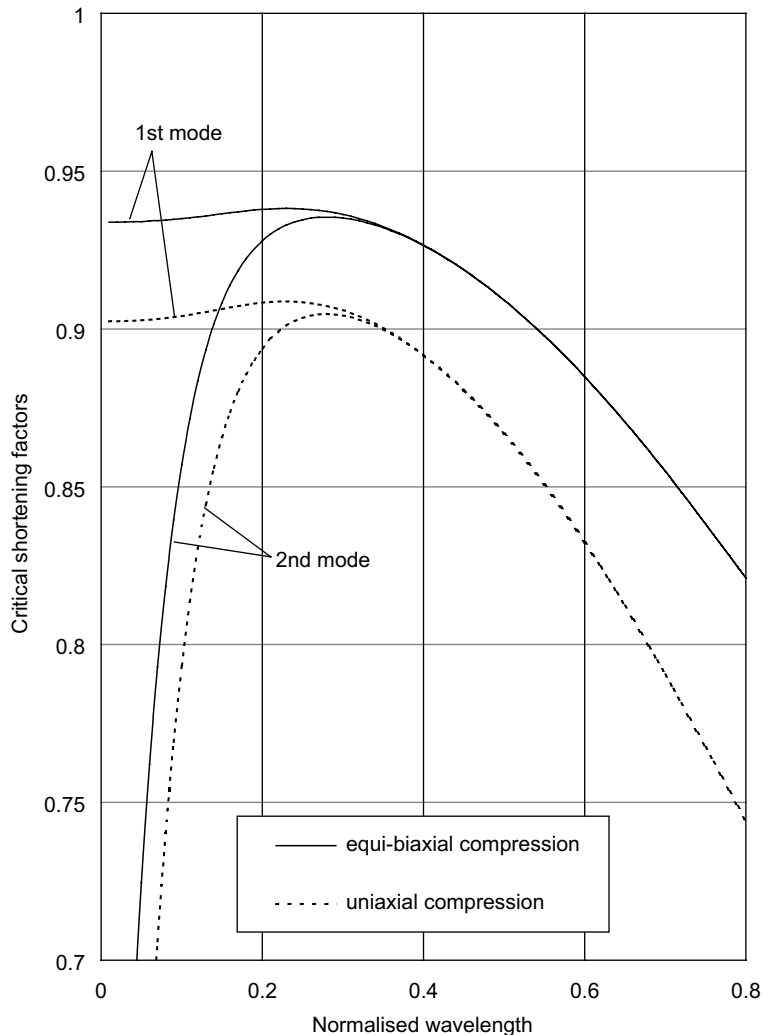


Fig. 4. Solutions of the characteristic equations; the shortening factor ( $\lambda_1$ ) is plotted against the normalised wavelength ( $\alpha_r$ ) for the case of  $C_{10}^r/C_{10}^m = 24$ ,  $h_r/h_m = 0.11$ .

#### 4. Accuracy of the continuum theory for the particular model of layers

##### 4.1. Hyperelastic layers

In this section, the accuracy of the continuum theory is considered for a composite material consisting of alternating non-linear elastic isotropic incompressible layers with different properties (Fig. 1a). Suppose that the materials of these layers are hyperelastic, Eq. (6), and the simplified version of the Mooney's potential, namely the so-called neo-Hookean potential, may be chosen for their description in the following form:

$$\Phi^r = 2C_{10}^r I_1^r(\varepsilon_{ij}^0), \quad \Phi^m = 2C_{10}^m I_1^m(\varepsilon_{ij}^0), \quad (28)$$

where  $\Phi$  is the strain energy density function (elastic potential),  $C_{10}$  is a material constant, and  $I_1(\varepsilon)$  is the first algebraic invariant of the Cauchy-Green strain tensor. This potential is also called the Treloar's potential, after the author who obtained it from an analysis of a model for rubber regarded as a macromolecular network structure made of very long and flexible interlinking chains (Treloar, 1975).

Taking into account the type of applied loads (Fig. 1a), the shortening factors in the plane of layers are

$$\lambda_1^r = \lambda_1^m = \lambda_2^r = \lambda_2^m \equiv \lambda_1. \quad (29)$$

The condition of incompressibility, Eq. (4), gives

$$\lambda_3^r = \lambda_3^m = \lambda_1^{-2}. \quad (30)$$

Then for the case of equi-biaxial compression, the components of the tensor  $\kappa_{ij\alpha\beta}$  for this model are expressed, according to Eqs. (1), (4)–(6), (28)–(30), as

$$\begin{aligned} \kappa_{1111}^r &= 2C_{10}^r(1 + \lambda_1^{-6}), & \kappa_{3333}^r &= 4C_{10}^r, \\ \kappa_{1313}^r &= 2C_{10}^r\lambda_1^{-3}, & \kappa_{1331}^r &= \kappa_{3113}^r = 2C_{10}^r, & \kappa_{1133}^r &= 0, \\ \kappa_{1111}^m &= 2C_{10}^m(1 + \lambda_1^{-6}), & \kappa_{3333}^m &= 4C_{10}^m, \\ \kappa_{1313}^m &= 2C_{10}^m\lambda_1^{-3}, & \kappa_{1331}^m &= \kappa_{3113}^m = 2C_{10}^m, & \kappa_{1133}^m &= 0, \end{aligned} \quad (31)$$

and, therefore, it follows from Eqs. (9) and (1), that

$$\xi_1^r = 1, \quad \xi_2^r = 1, \quad \xi_3^r = \lambda_1^6, \quad \xi_1^m = 1, \quad \xi_2^m = 1, \quad \xi_3^m = \lambda_1^6. \quad (32)$$

Substitution of Eqs. (31) and (32) into Eqs. (20) and (21) yields the asymptotic for the characteristic equations for the considered materials of the layers. As it was proved in the previous section, the solution of Eq. ce:cross-ref refid="fd18">>(20) will correspond to the result of the continuum theory.

On the other hand, substituting Eqs. (31) and (32) into the characteristic equation, Eq. (14), derived for the particular mode of stability loss within the most accurate approach, a transcendental equation is deduced. For each of the modes we have a different characteristic equation in terms of two variables,  $\lambda_1$  (shortening factor) and  $\alpha_r$  (normalised wavelength). After some transformations, the characteristic equation becomes:

- for the first mode (Fig. 2), from Eqs. (14), (15), (31) and (32),

$$\begin{aligned} & -\lambda^{-3}(1 + \lambda_1^6)^2[1 - C_{10}^r(C_{10}^m)^{-1}]^2 \tanh \alpha_r \lambda_1^{-3} \tanh \alpha_m \lambda_1^{-3} - 4\lambda_1^3[1 - C_{10}^r(C_{10}^m)^{-1}]^2 \tanh \alpha_r \tanh \alpha_m \\ & + [2 - (1 + \lambda_1^6)C_{10}^r(C_{10}^m)^{-1}]^2 \tanh \alpha_r \lambda_1^{-3} \tanh \alpha_m + [1 + \lambda_1^6 - 2C_{10}^r(C_{10}^m)^{-1}]^2 \tanh \alpha_r \tanh \alpha_m \lambda_1^{-3} \\ & + (1 - \lambda_1^6)^2 C_{10}^r(C_{10}^m)^{-1}(\tanh \alpha_r \tanh \alpha_r \lambda_1^{-3} + \tanh \alpha_m \tanh \alpha_m \lambda_1^{-3}) = 0; \end{aligned} \quad (33)$$

- for the second mode (Fig. 3), from Eqs. (14), (16), (31) and (32),

$$\begin{aligned} & -\lambda^{-3}(1 + \lambda_1^6)^2[1 - C_{10}^r(C_{10}^m)^{-1}]^2 \tanh \alpha_r \lambda_1^{-3} \coth \alpha_m \lambda_1^{-3} - 4\lambda_1^3[1 - C_{10}^r(C_{10}^m)^{-1}]^2 \tanh \alpha_r \coth \alpha_m \\ & + [2 - (1 + \lambda_1^6)C_{10}^r(C_{10}^m)^{-1}]^2 \tanh \alpha_r \lambda_1^{-3} \coth \alpha_m + [1 + \lambda_1^6 - 2C_{10}^r(C_{10}^m)^{-1}]^2 \tanh \alpha_r \coth \alpha_m \lambda_1^{-3} \\ & + (1 - \lambda_1^6)^2 C_{10}^r(C_{10}^m)^{-1}(\tanh \alpha_r \tanh \alpha_r \lambda_1^{-3} + \coth \alpha_m \coth \alpha_m \lambda_1^{-3}) = 0. \end{aligned} \quad (34)$$

#### 4.2. Results and discussion

The shortening factor,  $\lambda_1$ , is related to the value of strain,  $\varepsilon_{11}^0$ , by Eq. (1). As a result of solving the characteristic equations for different modes of stability loss, the dependences  $\lambda_1^{(1)}(\alpha_r)$  and  $\lambda_1^{(2)}(\alpha_r)$  are obtained

for the first and the second modes, respectively. The example of the dependences for equi-biaxial compression is given in Fig. 4 in comparison with the case of uniaxial compression. The latter case was considered following the solutions presented by Guz (1992) and Babich et al. (2001). The critical value for the particular mode,  $\lambda_{\text{cr}}^{(1)}$  or  $\lambda_{\text{cr}}^{(2)}$ , can be found as a maximum of the corresponding curve. The maximum of these values will be the critical shortening factor of the internal instability for the considered layered material determined by the most accurate approach,  $\lambda_{\text{cr}}$ ,

$$\lambda_{\text{cr}} = \max \left\{ \lambda_{\text{cr}}^{(1)}, \lambda_{\text{cr}}^{(2)} \right\} = \max \left\{ \max_{\alpha_r} \lambda_1^{(1)}, \max_{\alpha_r} \lambda_1^{(2)} \right\}. \quad (35)$$

Note that maximum shortening factors correspond to minimal strains and, therefore, to minimal loads according to Eq. (1).

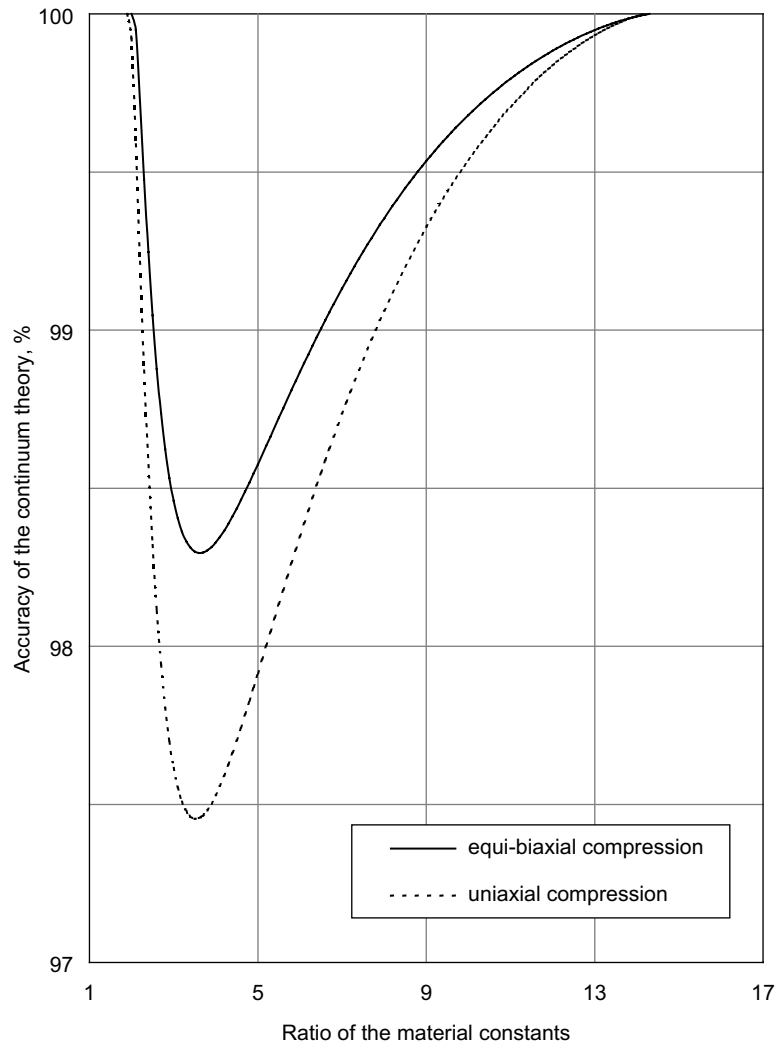


Fig. 5. The continuum theory accuracy ( $A$ ) as a function of the ratio of material constants ( $C_{10}^r/C_{10}^m$ ) for the cases of equi-biaxial and uniaxial compression;  $h_r/h_m = 0.16$ .

In the same time, according to the previous section, the shortening factor  $\lambda_1^{(1)}(\alpha_r)$  calculated for the first mode, corresponds to that of the continuum theory,  $\lambda_{c.t.}$ , when  $\alpha_r \rightarrow 0$ . Therefore, the accuracy of the continuum theory  $\Lambda$  (i.e. the ratio of the results obtained in the context of the most accurate approach and the continuum theory expressed in percentage) will be

$$\Lambda = \frac{\lambda_{c.t.}}{\lambda_{cr}} \times 100\% = \frac{\lim_{\alpha_r \rightarrow 0} \lambda_1^{(1)}(\alpha_r)}{\max \left\{ \lambda_{cr}^{(1)}, \lambda_{cr}^{(2)} \right\}} \times 100\% = \frac{\lim_{\alpha_r \rightarrow 0} \lambda_1^{(1)}(\alpha_r)}{\max \left\{ \max_{\alpha_r} \lambda_1^{(1)}, \max_{\alpha_r} \lambda_1^{(2)} \right\}} \times 100\%. \quad (36)$$

The values of  $\Lambda$  are presented in [Figs. 5 and 6](#) as functions of the ratio of the material constants,  $C_{10}^r/C_{10}^m$ . The results for equi-biaxial compression are given in comparison with uniaxial compression. All results

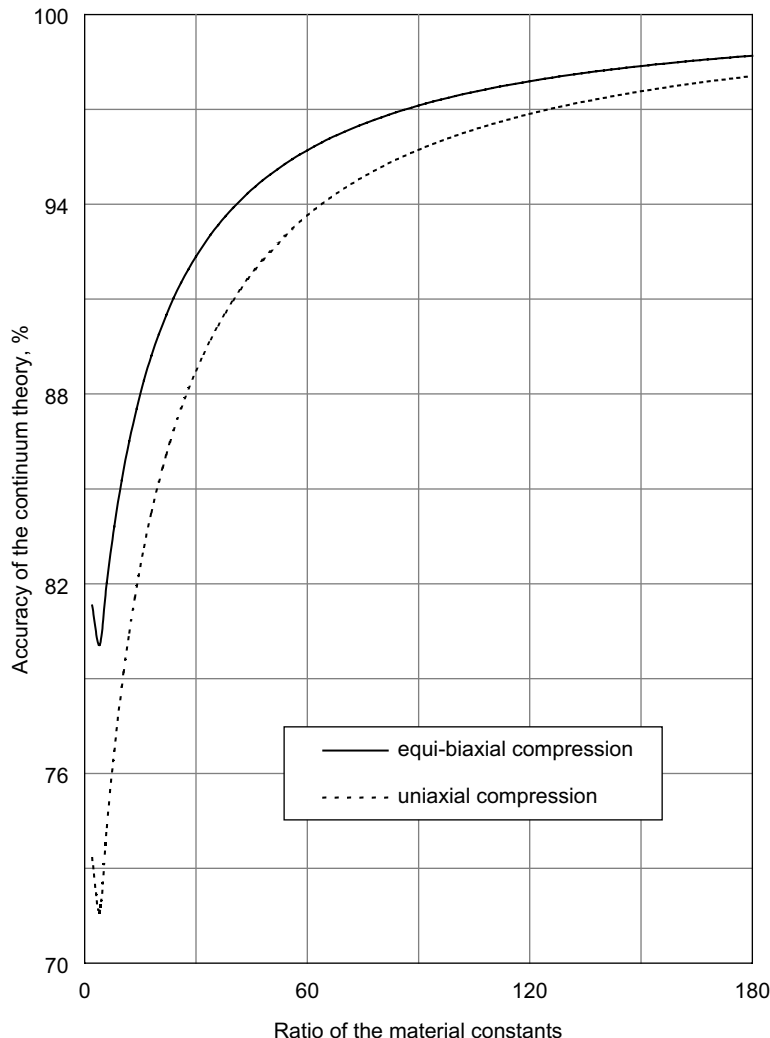


Fig. 6. The continuum theory accuracy ( $\Lambda$ ) as a function of the ratio of material constants ( $C_{10}^r/C_{10}^m$ ) for the case of equi-biaxial and uniaxial compression;  $h_r/h_m = 0.03$ .

corresponding to uniaxial compression are calculated following (Guz and Soutis, 2001b), where this case of loading was considered in detail. It should be noted that for plotting each point of the curves, the plots, similar to those in Fig. 4, are to be calculated and analysed.

One can see that the ratio of the material constants affects very much the accuracy of the continuum theory. The dependences in Figs. 5 and 6 have a strongly non-monotonous and non-linear character proving the importance of taking into account the material non-linearity. The volume fraction of layers has much stronger impact on the implementation of the continuum theory than any other physical or geometrical property of the composite. The increase in the volume fraction of the stiffer layer makes the continuum theory more accurate—the larger the layer thickness ratio  $h_r/h_m$ , the higher is the value of  $\Lambda$ . The type of loading (i.e. equi-biaxial or uniaxial compression) also affects the accuracy of the continuum theory, making it lower for the case of uniaxial compression. Of course, the actual magnitude of the critical loads for stability loss will also depend on the type of loading. It can be seen in Fig. 4, where the shortening factors for uniaxial compression are higher than for equi-biaxial compression. This is not surprising, since under equi-biaxial compression the composite experiences higher overall loads than in the case of uniaxial compression of the same intensity; and the internal instability will occur at lower strains (or higher shortening factors according to Eq. (1)).

Thus, based on the presented analysis, the accuracy of the continuum theory can be calculated for particular models of the layers. First, values of critical loads/strains are calculated within the scope of the most accurate (“exact”) approach (the piecewise-homogeneous medium model). Then comparing these critical values with the results of the continuum theory, the accuracy of the latter can be estimated for the particular layered materials and the conclusions about using this theory can be properly made.

## 5. Conclusions

Two methods of analysis of compressive strength of layered materials were discussed, assuming that the structure is still in a pre-buckling state: the continuum approach and the piecewise-homogeneous medium model. Two different loading conditions were compared: biaxial and uniaxial compression. Based on the results obtained within the scope of the model of a piecewise-homogeneous medium and the three-dimensional stability theory, the accuracy of a continuum theory was examined. The asymptotic accuracy of the continuum theory of compressive fracture was established for materials consisting of incompressible non-linear elastic transversally isotropic layers undergoing finite (large) deformations. It was rigorously proved, that the results of the continuum theory follow as a long-wave approximation from those for the first (shear) mode of stability loss obtained using the piecewise-homogeneous medium model.

The effect of the multi-axiality of loading on the accuracy of the continuum theory was determined for the particular model of hyperelastic layers described by the elastic potential of the neo-Hookean type (Treloar's potential). Estimation of accuracy was obtained by comparing the results of the continuum theory with the values of critical loads calculated within the scope of the most accurate approach (the piecewise-homogeneous medium model).

## References

- Babich, I.Yu., Guz, A.N., Chekhov, V.N., 2001. The three-dimensional theory of stability of fibrous and laminated materials. *International Applied Mechanics* 37 (9), 1103–1141.
- Biot, M.A., 1965. Mechanics of Incremental Deformations. Wiley, New York.
- Brekhovskikh, L.M., 1960. Waves in Layered Media. Academic Press, New York.
- Budiansky, B., Fleck, N.A., 1994. Compressive kinking of fibre composites: a topical review. *Applied Mechanics Reviews* 47 (6), S246–S270.

Camponeschi Jr., E.T., 1991. Compression of composite materials: a review. In: O'Brien, T.K. (Ed.), *Composite Materials: Fatigue and Fracture*, vol. 3, ASTM STP 1110, Philadelphia, PA, pp. 550–578.

Dow, N.F., Grunfest, I.J., 1960. Determination of most needed potentially possible improvements in materials for ballistic and space vehicles. General Electric Co., Space Sci. Lab, TISR 60 SD 389.

Guynn, E.G., Bradley, W.L., Ochoa, O., 1992. A parametric study of variables that affect fibre microbuckling initiation in composite laminates: Part 1—Analyses, Part 2—Experiments. *Journal of Composite Materials* 26 (11), 1594–1627.

Guz, I.A., 1989. Spatial nonaxisymmetric problems of the theory of stability of laminar highly elastic composite materials. *Soviet Applied Mechanics* 25 (11), 1080–1085.

Guz, A.N., 1990a. *Mechanics of Fracture of Composite Materials in Compression*. Naukova Dumka, Kiev.

Guz, I.A., 1990b. Continuum approximation in three-dimensional nonaxisymmetric problems of the stability theory of laminar compressible composite materials. *Soviet Applied Mechanics* 26 (3), 233–236.

Guz, A.N. (Ed.), 1992. *Micromechanics of composite materials: focus on Ukrainian research*. *Applied Mechanics Reviews* 45 (2), 15–101.

Guz, A.N., 1999. *Fundamentals of the Three-Dimensional Theory of Stability of Deformable Bodies*. Springer-Verlag, Berlin, Heidelberg.

Guz, A.N., Guz, I.A., 2003. Towards publications on brittle fracture mechanics of materials with initial stresses. *International Applied Mechanics* 39 (7).

Guz, I.A., Soutis, C., 2001a. A 3-D stability theory applied to layered rocks undergoing finite deformations in biaxial compression. *European Journal of Mechanics. A/Solids* 20 (1), 139–153.

Guz, I.A., Soutis, C., 2001b. Compressive fracture of non-linear composites undergoing large deformations. *International Journal of Solids and Structures* 38 (21), 3759–3770.

Korzh, V.P., Chekhov, V.N., 2002. Surface instability of laminated materials of regular structure under triaxial compression. *International Applied Mechanics* 38 (9), 1119–1124.

Niu, K., Talreja, R., 2000. Modelling of compressive failure in fiber reinforced composites. *International Journal of Solids and Structures* 37 (17), 2405–2428.

Papamichos, E., Vardoulakis, I., Muhlhaus, H.-B., 1990. Buckling of layered elastic media: a Cosserat-continuum approach and its validation. *International Journal of Numerical and Analytical Methods in Geomechanics* 14, 473–498.

Rosen, B.W., 1965. Mechanics of composite strengthening. In: *Fiber Composite Materials*. American Society of Metals Seminar, Ohio, pp. 37–75 (Chapter 3).

Schultheisz, C., Waas, A., 1996. Compressive failure of composites, Parts I and II. *Progress in Aerospace Science* 32 (1), 1–78.

Soutis, C., 1996. Failure of notched CFRP laminates due to fibre microbuckling: a topical review. *Journal of Mechanical Behaviour of Materials* 6 (4), 309–330.

Soutis, C., Guz, I.A., 2001. Predicting fracture of layered composites caused by internal instability. *Composites Part A* 32 (9), 1243–1253.

Soutis, C., Turkmen, D., 1995. Influence of shear properties and fibre imperfections on the compressive behaviour of CFRP laminates. *Applied Composite Materials* 2 (6), 327–342.

Tkachenko, E.A., Chekhov, V.N., 2002. Stability of an elastic layer stack between two half-spaces under compressive loads. *International Applied Mechanics* 38 (11), 1381–1387.

Treloar, L.R.G., 1975. *The Physics of Rubber Elasticity*. Oxford University Press, England.

Vardoulakis, I., Sulem, J., 1995. *Bifurcation Analysis in Geomechanics*. Blackie Academic & Professional, Glasgow.